

# Sensitivity Analysis and Calibration of the Heat Source in Additive Manufacturing of AlNiCo Magnets

Fachinotti Victor D.<sup>1,a\*</sup>, Gouttebroze Sylvain<sup>1,b</sup>, Azar Amin S.<sup>2,c</sup>

<sup>1</sup>Metal Production and Processing, SINTEF Industry, Oslo, Norway

<sup>2</sup>3D-Components AS, Oslo, Norway

<sup>a\*</sup>victor.fachinotti@sintef.no, <sup>b</sup>sylvain.gouttebroze@sintef.no, <sup>c</sup>amin.azar@3d-components.co

\*corresponding author: victor.fachinotti@sintef.no

**Keywords:** sensitivity analysis, calibration, AM, magnetic material, AlNiCo alloy

**Abstract.** This paper presents an initial investigation into the numerical modeling of additive manufacturing processes for AlNiCo magnets. The research concentrated on calibrating the heat source parameters by utilizing previously published experimental results. The influence of laser power and scanning speed on the laser fusion of AlNiCo5 on SS 304 substrates was investigated through single track experiments. The geometries of the melt pools were measured and utilized as the foundation for model calibration. A two-step calibration methodology was adopted: (1) a simplified 2D model implemented in Octave was used for sensitivity analysis and parameter fitting; and (2) validation was performed using a 3D model within the commercial software Simufact Welding software. Parameters calibrated through 2D simulations could be directly transferred to the 3D context. However, while the calibration procedure enabled accurate fitting for individual tracks, it resulted in globally non-optimal parameters, suggesting that process parameters influence laser penetration depth.

## Introduction

Permanent magnets are key components in modern technologies such as electric motors, wind-turbine generators, sensors, and actuators. The strongest commercial magnets rely on rare-earth elements, whose supply chains face major geopolitical and sustainability risks. Among rare-earth-free alternatives, AlNiCo alloys stand out for their high temperature magnetic stability and reasonable performance. AlNiCo magnets are typically manufactured by employing slow and carefully controlled directional solidification before undergoing magnetic treatment.

Additive manufacturing (AM) offers a transformative route to produce permanent magnets with complex geometries, controlled microstructures, and minimal material waste. Unlike conventional casting or powder metallurgy, AM allows localized control of solidification and phase evolution, that can potentially enable tailored magnetic anisotropy and optimized internal architectures. Numerical modelling is crucial for exploring this multidimensional design space, although significant uncertainties persist regarding material properties and their behavior under AM conditions.

AlNiCo5 is known to be brittle, and initial testing has revealed that it often develops cracks easily. In addition, the magnetic performance is strongly affected by the material texture. The material's full potential is realized only when the grains are well aligned, a condition presently attained through the directional solidification process. Numerical modelling is a powerful tool to explore different process parameters and their consequences on key parameters such as the temperature gradient and the cooling rate at the melt pool surface which are commonly used to determine the processability window and the columnar to equiaxed transition. In addition, numerical modelling is essential to test and design laser patterns that enable the reduction of residual stress and crack formation.

The model parameters are often calibrated based on dedicated experiments. In this work, single-track LPBF experiments on various substrates provided melt pool measurements that are used to calibrate the numerical parameters required for process simulation and optimization. The initial section provides a concise overview of the material data and experimental procedures. Subsequently,

the chosen modelling software and heat source models are detailed. Lastly, the results of the calibration process are examined and discussed.

### Material and Experimental Results

This study focuses on AlNiCo5 magnetic material and its deposition on different substrates. The details of the experimental work have already been published [1], so only a quick summary is provided here. Gas-atomized AlNiCo5 metallic powder was used as the feedstock. The single-track experiments were performed using an LPBF machine equipped with a 500 W ytterbium-fiber laser operating at 1064 nm and a laser spot size of 80  $\mu\text{m}$  by Gargalis and his co-authors [1]. Material samples were placed in slots.

After the single scan trials were carried out, a cross section of the samples was analyzed with optical microscope to extract information on the shape of the melting zone as presented in Figure 1.

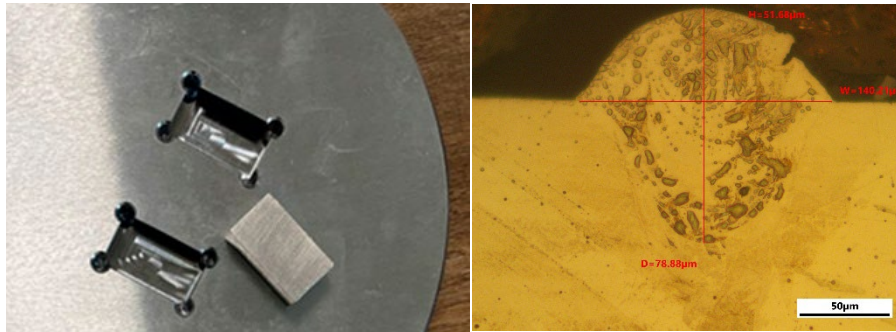


**Fig. 1.** Slot and material substrate (left) and measurement of the melting zone dimensions from experiments from [1].

**Table 1.** Design of experiment and single scan track processing parameters on AlNiCo5 and SS304 substrates.

High laser power				
Track #	Weld pool width ( $\mu\text{m}$ )	Weld pool depth ( $\mu\text{m}$ )	Power (W)	Scan speed (mm/s)
1	145.65	89.76	230	600
2	154.06	74.93	250	600
3	143.92	70.47	270	600
4	144.16	89.27	290	600
5	139.47	74.93	230	700
6	140.21	78.88	250	700
7	149.6	79.38	270	700
8	159.5	81.85	290	700
9	122.9	43.27	230	800
10	125.96	64.74	250	800
11	129.33	72.7	270	800

### Process Modelling

Simufact offers two software for additive manufacturing: Simufact Additive dedicated to a production perspective to predict and optimize building components, and Simufact Welding that allows for advanced heat source and melt pool simulations. Simufact Welding, version 2024.4, was selected for the following simulations as the melt pool is properly described. Single scan tracks of AlNiCo5 powder deposited on AlNiCo5 and AISI304 substrates via laser powder bed fusion (LPBF) are modelled. The powder bed is not explicitly represented in the simulation, only the added material

is present. The simulations are reproducing the experimental work done in the MagNEO project and summarized in the previous section and published [1] as seen in Figure 2. We focus on the AISI304 substrate due to available material property data (X5CrNi18-10\_sw in Simufact's database). The properties of AlNiCo5 materials are subject to considerable uncertainty, which will not be addressed in this work. To numerically study this point, a proper sensitivity analysis should be performed considering variations of key material properties (e.g. variations of a factor 4 for the conductivity, or +/- 100 K for melting point between different sources or CALPHAD simulations).

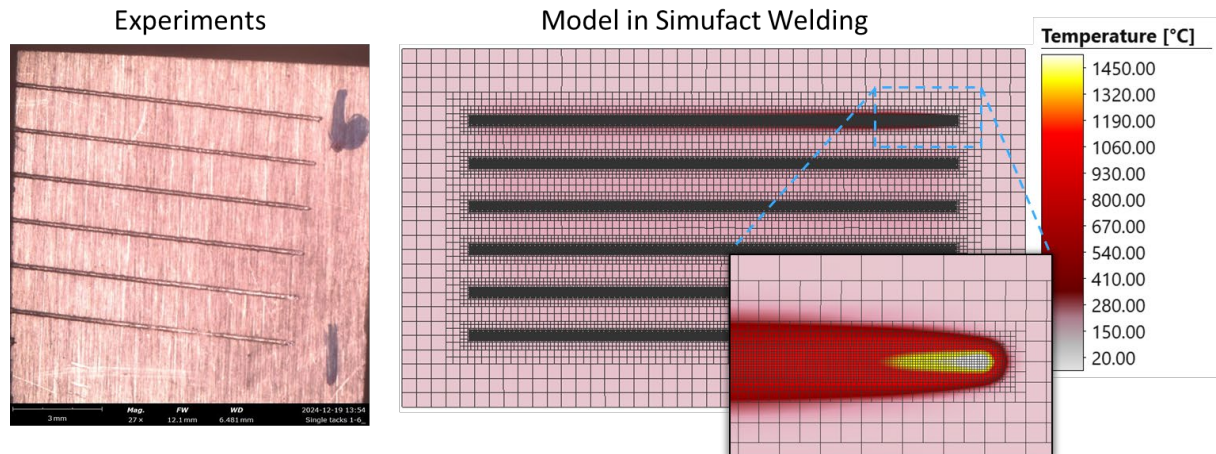


**Fig. 2.** Experiment [1] and simulation results from the high laser power deposition on AISI 304 substrate.

The heat source was defined using either a conical or a Goldak double-ellipsoidal model [2] as presented in Figure 3. The mesh refinement was activated around the heat source to properly capture the shape of the melting pool (minimum of 6 elements in the width).

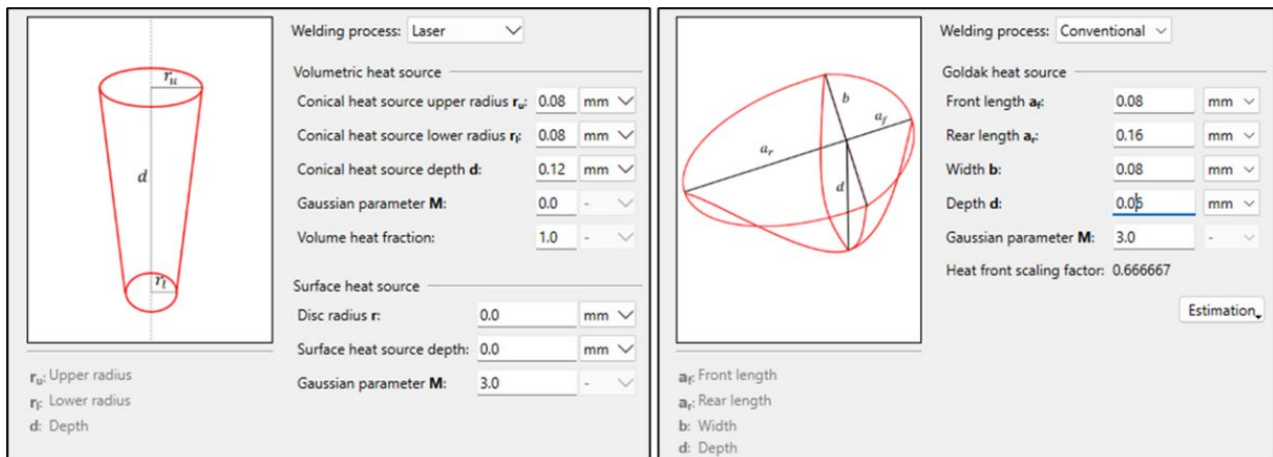


**Fig. 3.** Heat source models in Simufact Welding.

## Results

From a qualitative standpoint, comparison of the simulated and measured melt pool shapes (refer to Figure 4) demonstrates that the Goldak model more accurately captures the weld pool geometry observed in experiments. Although the conical model is commonly used for laser heat sources and has been recently identified as the most appropriate for LPBF [3], subsequent sections will focus exclusively on results obtained using the Goldak model.

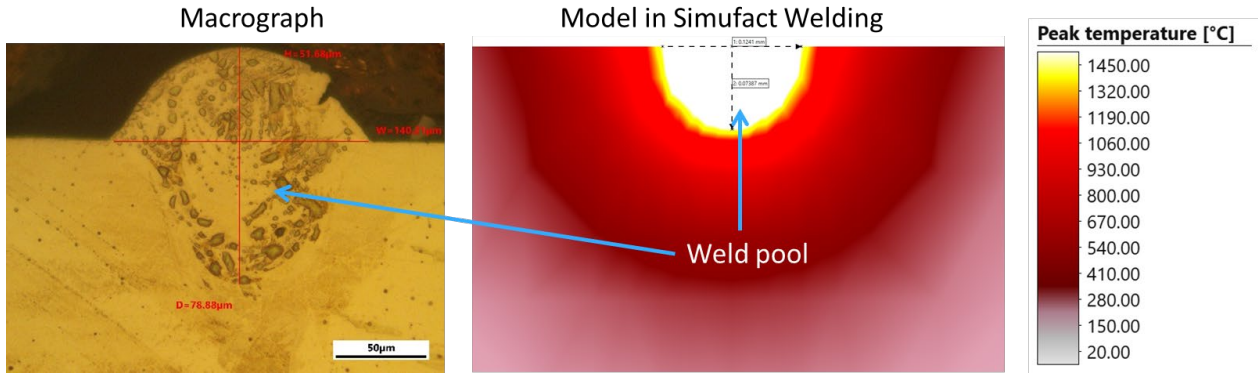


**Fig. 4.** Left: Observed weld pool in track 6, high laser power. Right: Corresponding weld pool estimation using Simufact Welding model with Goldak heat source.

As it can be seen on the right of Figure 3, the Goldak heat source is defined by five parameters: the dimensions  $b$  (half-width),  $d$  (depth),  $a_f$  (front length), and  $a_r$  (rear length) of the ellipsoids, and the Gaussian parameter  $M$ , which governs the distribution of heat within the ellipsoids. Following the original work of Goldak et al [2], we adopt  $M=3$  corresponding to a Gaussian distribution, and  $a_f = b/2$  and  $a_r = 2b$ , as they suggested in cases like these where there are no measures of the weld pool in the welding direction.

The error in weld pool prediction is assessed using Eq. (1):

$$\varepsilon = \max\left(\frac{|w_{\text{meas}} - w_{\text{mod}}|}{w_{\text{meas}}}, \frac{|d_{\text{meas}} - d_{\text{mod}}|}{d_{\text{meas}}}\right) \quad (1)$$

where  $w_{\text{meas}}$  and  $d_{\text{meas}}$  represent the measured width and depth of the weld pool, while  $w_{\text{mod}}$  and  $d_{\text{mod}}$  denote the corresponding values estimated using a finite element model. Then, we evaluate the sensitivity of this error to the remaining Goldak parameters ( $b$  and  $d$ ), as well as four other parameters with uncertain values: welding heat source efficiency  $\eta$ , the distance from the heat source center to the surface  $y_0$ , the heat convection coefficient with the environment  $h$ , and the ambient temperature  $T_\infty$ .

Constructing a sufficiently large sample for sensitivity analysis and calibration using the Simufact 3D finite element model is not feasible due to prohibitive computational time requirements. Consequently, we developed a simplified two-dimensional heat conduction model of the cross-section capable of estimating weld pool extension for any specified set of heat source parameters within seconds. This model was adapted for compatibility with Octave [4], a free open-source platform, based on the Matlab code previously utilized by Fachinotti and colleagues for welding [5] and additive manufacturing [6] applications. The accuracy of this two-dimensional cross-sectional approximation relative to the full 3D model is discussed in Ref. [5].

A sample containing 600 normalized sets of parameters  $[\eta, b, d, y_0, h, T_\infty]$  is built using the Octave's function `stk_sampling_maximinlhs` within the package STK [7], that implements the maximin Latin Hypercube method [8]. For each set, the weld pool is predicted for 24 cases with measured weld pool under different scan speeds and heat power, including all the cases listed in Table 1.

A classical regression-based sensitivity analysis commonly used in engineering design and uncertainty studies [9] is performed by taking the previous results as input. The linear and quadratic sensitivities of the error in predicting the weld pool, Eq. (1), to each parameter is shown in Figure 5. Three parameters are clearly the most important in the numerical prediction of the weld tool, and will be kept for calibration:  $\eta$ ,  $b$  and  $d$ .

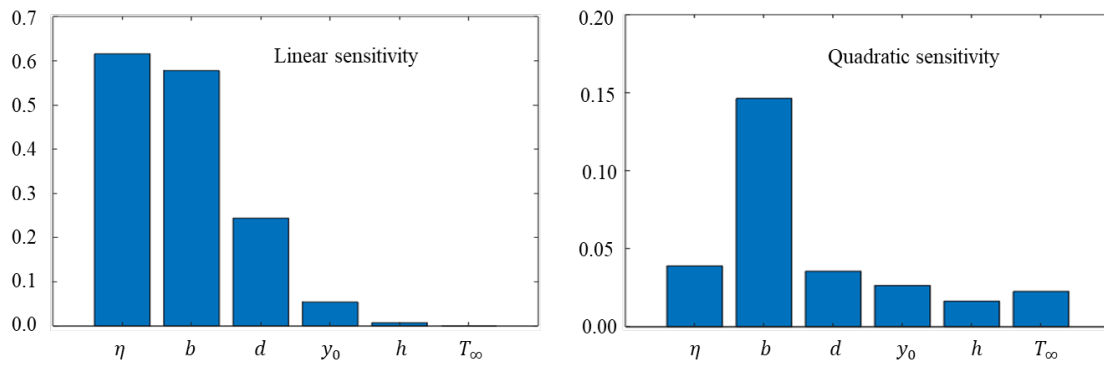


**Fig. 5.** Linear and quadratic sensitivities of the error in predicting the weld pool with respect to heat source efficiency ( $\eta$ ), Goldak's parameters ( $b$ : half-width, and  $d$ : depth), distance from the heat source center to the surface ( $y_0$ ), heat convection coefficient to the environment ( $h$ ) and environment temperature ( $T_\infty$ ).

Calibration is performed using a new maximin Latin Hypercube sample containing 600 normalized sets of parameters  $[\eta, b, d]$ , generated once again with Octave's function `stk_sampling_maximinlhs`. First, in an attempt to determine a unique heat source, the weld pool was predicted for all the high-power tracks listed in Table 1 and for each set  $[\eta, b, d]$ . Unfortunately, not one single set works satisfactorily well for all the tracks, so we decided to perform calibration for each individual track. Now, the numerical results obtained using the simplified 2D cross sectional model match the experimental observations satisfactorily (see Figure 6). Let us remark that similar melt pool dimensions were obtained when running the full 3D model in Simufact Welding as illustrated in Figure 7 for track 6.

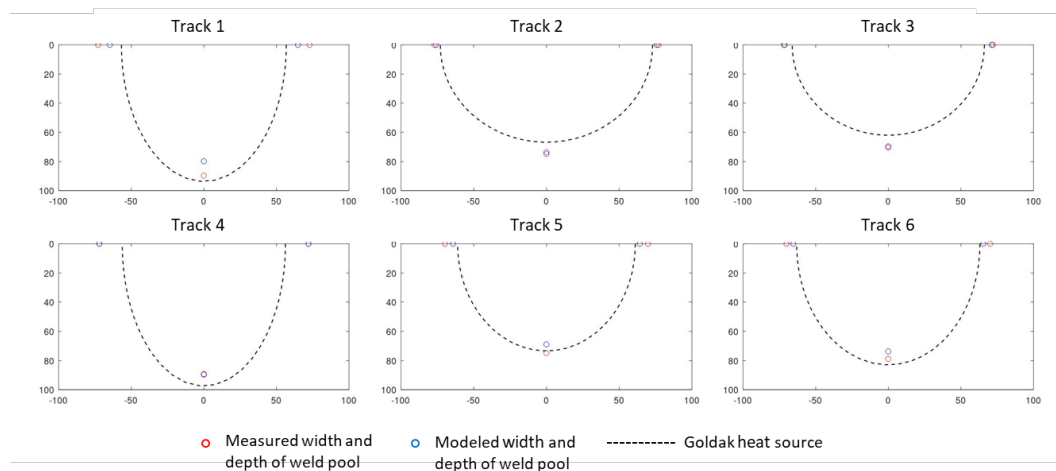


**Fig. 6.** Measured weld pool width and depth compared to results obtained using Simufact Welding with Goldak heat source for the tracks 1 to 6 deposited with high laser power.

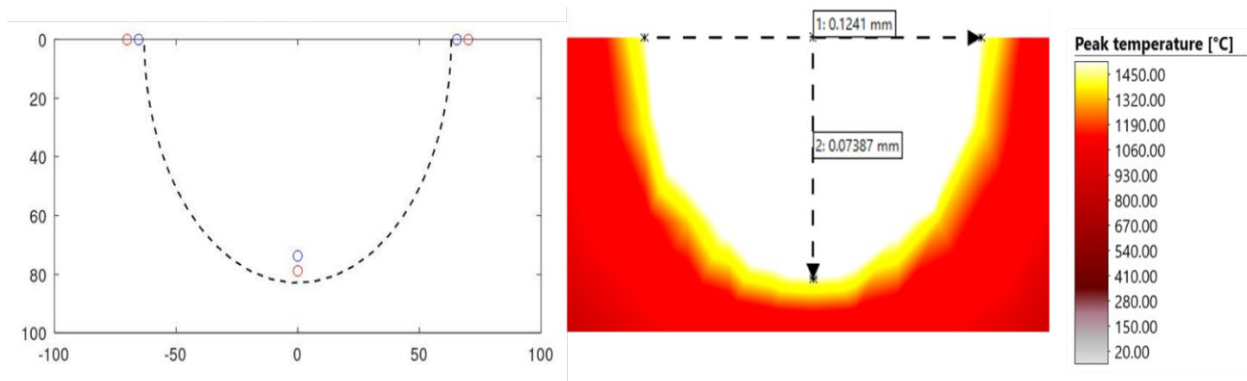


**Fig. 7.** Comparison of Octave melt pool shape and Simufact cross-section for high power track 6.

Table 2 lists the sets of calibrated Goldak's parameters for each track, and the agreement of numerical predictions with experimental observations, quantified by the error defined by Eq. (1(1)). The values of the parameters vary significantly and without a clear trend.

**Table 2.** Results of individual and global calibration for high laser power.

Track #	$a_f$ [ $\mu\text{m}$ ]	$a_r$ [ $\mu\text{m}$ ]	$b$ [ $\mu\text{m}$ ]	$d$ [ $\mu\text{m}$ ]	Error
1	28.4	113.61	56.8	93.7	0.1099
2	36.5	146.0	73.0	66.8	0.0155
3	33.1	132.4	66.2	62.0	0.0116
4	28.1	112.4	56.2	97.5	0.0041
5	30.5	122.2	61.1	73.4	0.0800
6	31.5	126.2	63.1	83.0	0.0674

Some intrinsic variability is expected in such process, but the process study requires the prediction of the source parameters based on the process parameters. Therefore, a response surface should be developed to define the Goldak source as a function of both its intrinsic parameters and process variables such as scan speed and laser power, factors often missing in calibration studies reported in the literature (e.g., [10]).

## Conclusion

In this work, a two-step modelling approach was implemented to decouple heavy 3D modelling from the heat source calibration. This strategy enabled a successful calibration of the model parameters at the level of individual laser tracks, demonstrating the capability of the approach to reproduce the experimentally measured melt pool for one testing substrate. Nevertheless, the global calibration does not generate a unique set of parameters that can be used in the power and scanning speed design domain. While the results confirm the relevance and robustness of the proposed methodology for single-track analysis, further work is required to predict the heat source parameters toward truly process-dependent quantities. One solution could be to obtain implicit relations between process parameters and source parameters using a machine learning algorithm. Additional data covering not only single tracks, but also multiple layers deposition needs to be included in future study to correlate the residual stress calculation with the crack occurrence to analyze the effect of the different patterns. Measurements of the melt pool dimensions during a multi-layer deposition will also enable the extension of the calibration of the source in a future work.

## Acknowledgement

The authors would like to thank the European Union for the funding received for the HEU MagNEO project (grant agreement ID: 101130095).

## References

- [1] L. Gargalis, L. Karavias, A. Argyrou, E.K. Karaxi, E.P. Koumoulos, Additive Manufacturing of AlNiCo5 Hard Magnetic Alloy Through Laser Powder Bed Fusion: A Single Scan Track Study of Microstructure and Nanomechanical Integrity, *Appl. Sci.* 15(23) (2025), doi: 10.3390/app152312522.
- [2] J. Goldak, A. Chakravarti, M. Bibby, A new finite element model for welding heat sources, *Metallurgical Transactions B*, Vol. 15B, 299-305, 1984.
- [3] M. Kusano, M. Watanabe, Heat Source Model Development for Thermal Analysis of Laser Powder Bed Fusion Using Bayesian Optimization and Machine Learning, *Integrating Materials and Manufacturing Innovation* (2024) 13:288–304, doi: 10.1007/s40192-023-00334-2.

- 
- [4] J.W. Eaton, D. Bateman, and S. Hauberg, R. Wehbring, GNU Octave version 9.2.0 manual: a high-level interactive language for numerical computations (2024), <https://www.gnu.org/software/octave/doc/v9.2.0>.
  - [5] V.D. Fachinotti, A.A Anca, A. Cardona, Analytical solutions of the thermal field induced by moving double-ellipsoidal and double-elliptical heat sources in a semi-infinite body. *International Journal for Numerical Methods in Biomedical Engineering* 27 (2011) 595–607.
  - [6] V.D. Fachinotti, A. Cardona, B. Baufeld, O. Van der Biest. Finite-element modelling of heat transfer in shaped metal deposition and experimental validation. *Acta Materialia* 60 (2012) 6621–6630.
  - [7] J. Bect, E. Vazquez. STK: a Small (Matlab/Octave) Toolbox for Kriging. Release 2.8.1 (2023). <https://github.com/stk-kriging/stk>.
  - [8] D. Morris, T.J. Mitchell. Exploratory designs for computational experiments. *Journal of Statistical Planning and Inference* 43 (1995) 381–402.
  - [9] D.C. Montgomery. *Design and Analysis of Experiments*. 9th Edition, Wiley (2020).
  - [10] G. Ertugrul, A. Hälsig, R. Rimpl, J. Hensel, S. Härtel, Artificial neural network based calibration of Goldak heat source parameters in tandem plasma transferred arc process using finite element analysis, *Int. J. Adv. Manuf. Tech.* 139 (2025), 2349-2363, doi: 10.1007/s00170-025-15843-x.